Integration of Fuel Cell Technologies in Renewable-Energy-Based Microgrids Optimizing Operational Costs and Durability

L. Valverde, C. Bordons, *Member, IEEE*, F. Rosa

***Abstract*—In this paper, a Model Predictive Control (MPC) approach is proposed to manage a grid-tied hydrogen microgrid. The microgrid testbed is equipped with a 1kW PEM electrolyzer and a 1.5 kW PEM fuel cell as main equipment. In particular, we present a formulation that includes the cost of the electricity exported/imported, the aging of the components and the operational constraints. The control objective is to satisfy user demand as well as extend the lifespan of expensive equipment as is the case of the fuel cell or the electrolyzer. Microgrid performance is investigated under realistic scenarios in three experiments. The experimental results illustrate how the proposed control system is able to manage the fuel cell and the electrolyzer through smooth power references as well as to satisfy the power demanded. Finally, benchmarking is carried out between Hysteresis Band (HB) control and the proposed MPC in regards to efficiency and cost of the operation. The results obtained show that the MPC approach is more effective than HB for this type of microgrid, with a reduction in operation cost of up to 30%.**

***Index Terms*— Energy storage, fuel cell, hydrogen, microgrid, model predictive control, power management, renewable.**

NOMENCLATURE

C	Associate cost for degradation (€)
$G_{battery}$	Transfer function for the battery bank
G_{ez}	Transfer function for the electrolyzer
G_{fc}	Transfer function for the fuel cell
HB	Hysteresis Band
I^*	low frequency battery current dynamics (A)
I_{chr}	battery charging current (A)
I_{dis}	battery discharging current (A)
J	Cost function
KPI	Key Performance Indicators
MHL	Metal Hydride Level (%)
m_{Hnet}	hydrogen flow rate (Nl/min)
MPC	Model Predictive Control
N	Prediction horizon
Nu	Control horizon
P	Electrical power (W)
PEM	Polymer Electrolyte Membrane
PV	Photovoltaic
ref	Reference
RES	Renewable Energy Source
SOC	Battery State Of Charge (%)
Ts	Sampling time (s)
WT	Wind turbine
x	System state
u	Control actions
x_{b1}	Sunny day state
x_{b2}	Cloudy day state
x_{b3}	Windy day

Subscripts and superscripts:

ez	Electrolyzer
$batt$	Battery
dem	Demand
dP	Power variation
fc	Fuel cell
$grid$	Electrical grid
max	Maximum value
min	Minimum value
$O\&M$	Operation and maintenance cost
$On\text{-}off$	Equipment switch on-off
Voc	Open circuit voltage
wt	Wind turbine
$high$	Higher limit of power from renewables
net	Net power
gen	Generated

Greek symbols:

α_i	Weight for manipulated variables
β_i	Weight for the variation of manipulated variables
γ_i	Weight associate to the error of the outputs
δ^{PV}	Binary variable

Manuscript received November 24, 2014; revised March 2, 2015; June 5, 2015 and July 4, 2015; accepted July 22, 2015.

The authors acknowledge MINECO for funding this work under the project DPI2013-46912-C2-1-R.

L. Valverde and F. Rosa Authors are with the Energy Engineering Department, School of Engineering, University of Seville 41092, Seville, Spain (e-mail: lvalverde@etsi.us.es; rosaif@us.es).

C. Bordons is with the System engineering and automation, School of Engineering, University of Seville 41092, Seville, Spain (e-mail: bordons@etsi.us.es).

I. Introduction

THE adoption of Renewable Energy Sources (RES) has experienced a massive expansion in recent years. Challenges arise from the natural intermittency of RES and the requirement to satisfy uncertain user demand. Nowadays, growing interest in combining energy storage with RES is spurring this research field [1], [2]. As an energy carrier for stationary applications, the hydrogen microgrid concept relies on the production of hydrogen by means of electrolyzers (an industrial machine that uses the electrolysis principle), storing the hydrogen for long periods (compressed, liquated or in metal hydride) and producing electrical power with a fuel cell, consuming the hydrogen previously stored (and oxygen from air) with only water as a by-product. Although the feasibility of hydrogen for balancing renewable power (mainly photovoltaic and wind power) has been demonstrated, effective control of H_2-μGs remains a challenging undertaking, since it has often been neglected in pursuit of simplicity. Later experience demonstrated that μG performance is highly subject to the control strategy and has not been quite up to the mark [3], [4]. Furthermore, according to the literature, equipment lifespan strongly depends on the power and load profiles they are subjected to [5], [6], [7]. Authors agree that the most relevant issues were low operation efficiency (15-25% hydrogen round trip) and premature equipment degradation. These issues are considered to be related to the simplicity of energy management [8], [9], which nevertheless can provide acceptable results for relatively low RES penetration. However, simple control strategies have been demonstrated to be insufficient when high percentages of RES and multiple storage devices are incorporated into the system. Electrolyzers and fuel cells are a proven, reliable technology, but are still expensive and not specifically designed to cope with renewable energy and fast demand response. Hence, a suitable control strategy should include a diversity of parameters, such as cost optimization, equipment damage, etc., in addition to simply balancing the supply-demand equation, allowing dispatchable units to be maintained at their maximum efficiency and preventing or reducing the intensive use of expensive equipment. This is the motivation for the advanced control developed and implemented in the present work. Within advanced control techniques, Model Predictive Control (MPC) has been widely recognized as a popular control methodology for industrial and process applications [10]. Including operating constraints in the formulation makes MPC a very attractive technique for hydrogen microgrids. However, published works that employ this strategy in field applications of hydrogen μGs are scarce as opposed to those using well-established heuristic techniques, such as the Hysteresis Band control [11], [8], [12], [13].

Among the works available in the literature on using MPC for renewable μG control, the work by Zervas [14] presents an integrated framework for renewable power management. The framework is built in several steps, as is usual, to separate the time scales. In the first step, a Neural Network is used to predict the solar irradiance. The next step is the estimation of the power produced by a solar array. And finally the MPC provides the optimal decision strategy. A different approach can be found in the work of Khalid [15], where the MPC is implemented in a renewable energy network to smooth the wind power fluctuations. In this case, battery storage is used instead of hydrogen vector. The amounts of electrical power transferred to the network and batteries were considered to be the control variables. Del Real et al. [16] presented the implementation of an MPC for a hybrid solar plant model with fuel cell and hydrogen storage. Korpås [17] included day-ahead electricity market prices for the problem formulation, as well as a penalty cost for unprovided hydrogen in a hypothetical system where H_2 is used as a fuel. More recently, one can find a comprehensive power management approach for the hybrid renewable microgrid using MPC, with hydrogen and batteries as intermediate storage in [18]. Trifkovic [19] presented a low-level control system, comprising a central heuristic supervisory controller and local decentralized MPC controllers in a stand-alone microgrid located in Sarnia (Canada). A mixed integer linear framework for economic scheduling is incorporated in a MPC for optimizing a microgrid operation installed in Athens, Greece [20].

There are significant differences between these works and our approach. To the best of the authors' knowledge, no real-time controller for optimal μG dispatch has been developed so far. Moreover, nearly all the works available in the literature are only studied at simulation level, without delving into challenges and constraints, such as equipment degradation, that can be found in a real system. Only long-term scheduling has been tested in real plants. However, these approaches are generally very computationally demanding, and therefore are not suitable for real-time applications. Although these works are very relevant for simulation studies, they are not feasible for power management of real systems, and they may result in suboptimal solutions.

To address the aforementioned issues, we have developed a more suitable approach based on implicit-MPC formulation, capable of fast and effective calculation of optimal set-points for power management, but complex enough to take into account degradation and equipment constraints in the formulation. Time horizon was set to few seconds, which is more suitable for a real-time control, allowing fast response to sudden disturbances both in demand and renewable production. Hardware-in-the-loop is used in combination with real electrolyzer, fuel cell, batteries and hydrogen storage, to present a novel field integration application of fuel cell technologies into microgrids, optimizing cost and durability.

This paper is organized as follows: Section II is dedicated to describing the experimental setup. Section III states the MPC theoretical formulation for H_2-μG optimization. The results of experimental validation are shown in Section IV, while Section V is focused on discussion and benchmarking of the controller. Finally, Section VI summarizes the main study achievements and future work.

II. Microgrid System Description and Experimental Setup

The microgrid under study is an experimental renewable-energy-based microgrid platform installed at latitude 37.10 N. A picture of the system laboratory microgrid is shown in Fig. 1, where main components can be observed. The test bench comprises a 1 kW PEM electrolyzer, a 7 Nm^3 metal hydride hydrogen storage tank, a 1.5 kW PEM fuel cell and a 367 Ah lead-acid battery bank as main components. The renewable source is emulated by means of Hardware-in-the-Loop in a 6 kW DC electronic power supply. Likewise, a 2.5 kW DC electronic load emulates demand profiles (household, electric vehicles, industry, etc.). All this equipment is connected to a DC current bus with the necessary power electronics. To facilitate the understanding of the microgrid topology, a schematic representation of the system with electric and control signals is shown in Fig. 2. In this figure, it can be seen that the grid power exchange is also electronically emulated.

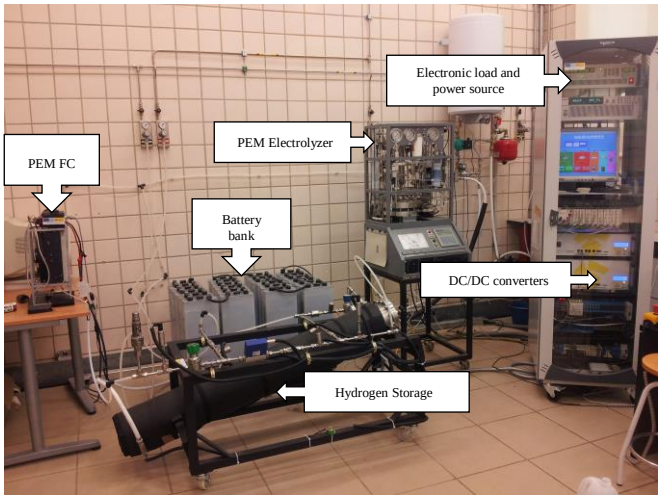

Fig. 1. Laboratory-scale microgrid comprising: electrolyzer, fuel cell, hydrogen storage (metal hydride alloy), battery bank, electronic power source and load.

With regard to the control system, the μG has a dedicated central control based on a programmable logic controller (PLC). This device performs the required calculations and determines the control actions. Power supply and electronic load are controlled analogically while the electrolyzer and fuel cell are controlled by means of the power converters and CAN bus communications. The fuel cell and the electrolyzer units have their own local controllers, which execute the signals received from the converters. Thus, a compromise between fully centralized and fully decentralized control architectures is achieved by means of the hierarchical control architecture.

Two DC/DC converters associated to the electrolyzer and fuel cell allow the DC bus to transfer power. In contrast, the battery bank is plugged to the DC bus directly. Hence, bus voltage is held by the battery bank, simplifying the topology. This is a common option in DC microgrids in order to reduce costs and increase reliability, as any unbalance in the system is absorbed by the batteries [13]. The converters associated with the renewable source and the demand are electronically emulated. A detailed description of the microgrid design and full characterizations of each subsystem can be found in [21].

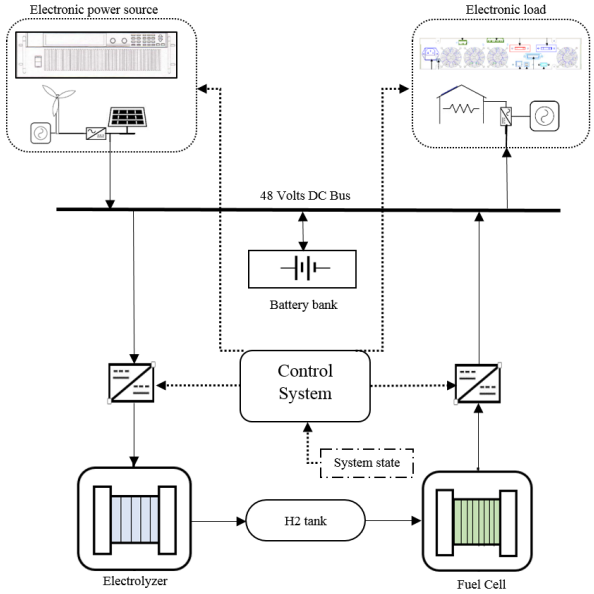

Fig. 2. Microgrid system Layout showing the main control signals (dotted arrows)

III. Formulation and Implementation of the Model Predictive Controller

In this section, the problem statement and control objectives are explained within the model predictive control formulation.

A. Control Objectives

The primary goal of the microgrid power management control is to ensure stable delivery of electrical power to its local load consumers. In addition to this, it encompasses performance optimization and prevents equipment damage. Specifically, the proposed control aims to fulfill the following objectives: 1) To protect the battery bank from deep discharging and overcharging. 2) To limit the electrolyzer and fuel cell power rates in order to protect such expensive equipment from intensive use. 3) To take into account the energy efficiency in the plant, i.e. using batteries as first energy storage means whenever possible. Since the H2 roundtrip efficiency is much lower than batteries' efficiency, this path is used only when there is a large imbalance between production and demand. 4) To provide flexibility in the operation, guaranteed by establishing gentle weights in the cost function for reference tracking. 5) To minimize the energy exchanged with the grid to achieve a high degree of autonomous operation.

In this multi-objective optimization problem, the goal is to achieve an optimal solution for several competing objectives. In such problems, the satisfaction of the cost function becomes a Pareto optimum where the solution represents a state of trade-off between objectives. Therefore, the microgrid will reach a state of energy resource allocation in which it is

impossible to make any one individual better off without making at least one individual worse off. Applied to a µG, one of the energy units will have to cope with ripples and/or sudden power changes. In our design, the grid has to cope with the rapid demand changes in order to protect the rest of the equipment from intensive use. This approach has been chosen from the microgrid user's point of view. The alternative approach, more favorable for the grid operator, is also possible.

B. Control Architecture and Approach

The control architecture proposed herein is presented in this section. Four manipulated variables manage the system: the fuel cell power production (P_{fc}), the electrolyzer power consumption (P_{ez}), the power exchange with the grid (P_{grid}) and the battery power (P_{batt}). Since in renewable energy systems the power generated and demanded will generally differ, the main objective of the proposed architecture is to calculate the reference signals for the manipulated variables in order to cope with the mismatch between the power generated and demanded.

As the control scheme in Fig. 3 shows, a disturbance has been added to the controller. This strategy allows inclusion of the power demanded and generated profiles in the scheme. Due to the fact that there is no dedicated power converter associated with the battery bank, which is therefore not directly controlled, this variable will be forced to zero by setting a high weight in the cost function. Then, using the rest of the manipulated variables (P_{ez}, P_{fc}, P_{grid}), the controller has to balance the mismatch between power generated and demanded, allocating the excess or deficit energy optimally among the microgrid units. If the battery is equipped with a dedicated power converter, then it is just considered to be one of the manipulated variables. During the operation, if possible, the controller keeps a certain amount of energy stored around the desired output references [SOC_{ref}, MHL_{ref}]. Curtailments of the renewable source have not been considered since the idea is to take full advantage of the renewable power.

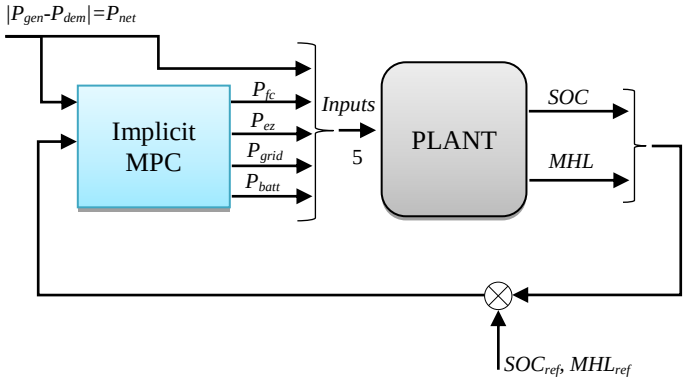

Fig. 3. Control scheme architecture proposed for managing the hybrid microgrid. *SOC*: Battery State of Charge, *MHL*: Metal Hydride Level, P_{fc}: fuel cell power, P_{ez}: electrolyzer power, P_{grid}: grid power, P_{batt}: battery power, P_{gen}: generated power, P_{dem}: demanded power, P_{net}: net power.

C. Control Layers and Hierarchy

Different control levels can be defined in a microgrid, depending on the time scale of the control actions [22]. Therefore, a logical approach is a hierarchical control structure. Fig. 4 shows the three main levels that have been defined in this work. The controller presented in this study is located in the second level, where the MPC calculates on-line optimal set- points, which are sent as control signals to the power converters. Then the fuel cell and the electrolyzer on-board electronic control units determine the best trajectory to reach the set-points, according to their own manufacturer's controller.

The first layer contains a weather detector block to identify typical weather patterns. At the beginning of the renewable energy production, the weather detector evaluates when the system is under stable solar irradiation or, in contrast, when it is under the characteristic high variability irradiation of the clouds. Acting as an MPC tuning, the weather detector allows switching between MPCs with different cost function weights. The multiple MPC permits different operation for each weather pattern. Such a layer makes possible to improve the control architecture shown in Fig. 3 by including a reference governor which gives the operation mode for the implicit MPC controller. In particular, this governor has three Boolean states $\{x_{b1}, x_{b2}, x_{b3}\}$, defined in table I. In a PV-µG, x_{b1} and x_{b2} correspond with the two possible weather scenarios (Sunny and Cloudy), while x_{b3} indicates when the wind turbine is producing power in a wind-based µG. The mathematical formulation of these states is presented below:

$$x_{b1}(k) = \neg\, \delta^{PV} \tag{1}$$

$$x_{b2}(k) = \delta^{PV} \tag{2}$$

$$x_{b3}(k) = P_{wt} > 0 \tag{3}$$

$$\delta^{PV} \begin{cases} 1 & \text{if } \left|\dot{P}_{PV}\right| \geq \dot{P}_{high} \\ 0 & \text{otherwise} \end{cases} \tag{4}$$

TABLE I
MODE SELECTOR

Pattern	mode
Sunny	Xb_1
Cloudy	Xb_2
Windy	Xb_3

δ^{PV} indicates when the solar power variation is higher than a pre-defined value ($\dot{P}_{high}$) which is characteristic of the stochastic behavior of the cloudiness. P_{wt} is the power produced by the wind turbine.

In the MPC layer in Fig. 4, three variants of the MPC controller can be implemented, optimized for each weather condition. Using this strategy, different operation modes can be obtained which are better suited to the changing character of the plant set-point and external conditions.

The second layer contains the implicit MPC responsible for the reliable, secure and economical operation of the microgrid. This task becomes particularly challenging in RES-H_2 µGs

with the presence of still-expensive technologies, such as fuel cells, where the dispatch command should be high enough to follow the sudden load changes while at the same time achieving certain objectives of their life cycle, which is highly dependent on the load profile.

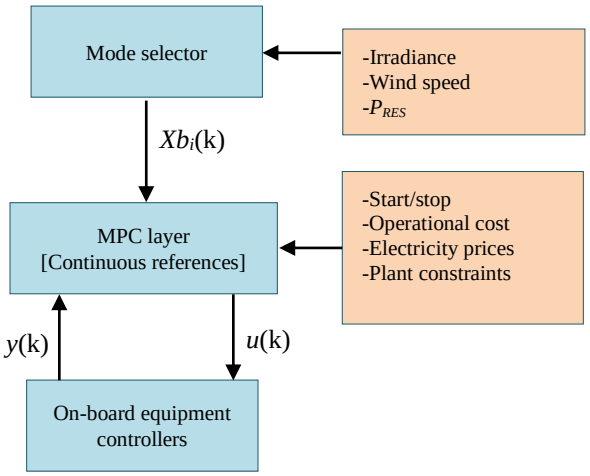

Fig. 4 . Schematic diagram of microgrid hierarchical control architecture

D. *Linearized Model for Prediction*

A control-oriented linear model is required by the controller to forecast the plant outputs. This model is drawn from a comprehensive non-linear one presented in [23]. A LTI system described by the following state-space representation is used:

$$\begin{aligned} \dot{x}_{k+1} &= A_d \cdot x_k + B_d \cdot u_k + B_d' w_k \\ y_k &= C_d \cdot x_k \end{aligned} \tag{5}$$

where k represents the sampling time, x(k) ϵ $\mathbb{R}^n$ represent the system states, u(k) ϵ $\mathbb{R}^m$ are the control actions (or manipulated inputs) and y(k) ϵ $\mathbb{R}^p$ are the controlled variables.
Before the linearization process, the state variables (x), system outputs (y) and control actions (u) are summarized below for clarity:

$$x(t) = \begin{pmatrix} I* \\ I_{chr} \\ I_{dis} \\ m_{Hnet} \end{pmatrix}(t);\quad u(t) = \begin{pmatrix} P_{fc} \\ P_{ez} \\ P_{grid} \\ P_{batt} \end{pmatrix}(t); y(t) = \begin{pmatrix} SOC \\ MHL \end{pmatrix}(t) \tag{6}$$

The model linearization comprises several steps. The first step involves choosing an arbitrary working point for the initial states of the batteries' State Of Charge, Metal Hydride Level and manipulated variables. In this case, the criterion was to select three different characteristic operating points of the three weather scenarios. The working points were set at 60%, 40% and 70% of SOC and 50% MHL, for the initial states of the Sunny, Partly Cloudy and Windy scenarios respectively. 500 W was selected for the fuel cell, as well as the electrolyzer power (which is in the middle of the equipment power range). Grid power was 200 W (imported power). The battery power was set to 1000 W (charging) and the disturbance P_{net} was 1000 W for the three scenarios.

The linear model has been obtained using standard Matlab® tools for linearization. The discrete linear model obtained using the Tustin method for discretizing the system can be expressed in the state of space, in the matrix form of (7).

$$\begin{aligned} x(k+1) &= x(k) + \\ &+ \begin{pmatrix} -0.02083 & 0.02083 & -0.02083 & -0.02083 \\ -2.003\times10^{-7} & 6.796\times10^{-8} & 0 & 0 \end{pmatrix} \cdot u(k) + \\ &+ \begin{pmatrix} -0.02083 \\ 0 \end{pmatrix} w(k) \\ y(k) &= \begin{pmatrix} -0.0001778 & 0 \\ 0 & 14.29 \end{pmatrix} x(k) \end{aligned} \tag{7}$$

It worth pointing out that the choice of a suitable sampling time is an important task in the controller design. Sampling time selection must be checked to ensure that the discretized model properly captures the system dynamics. In this case, a sampling time of 1 second was chosen to properly capture the dominant dynamics, which are on the order of seconds.

The control model obtained using the linear model representation is shown in Fig. 5 and it is composed of four main modules. The electrolyzer and the fuel cell modules in Fig. 5 are respectively considered to be a production and consumption of hydrogen with dependency proportional to the power. This is because linear behavior can be assumed for the electrolyzer and the fuel cell production/consumption near the working zone [16]. The hydrogen storage tank is considered to be a hydrogen mass balance, while the battery behaves as an integrator, as well, around the set-point. The plant outputs are the storage levels, SOC (State of Charge of the battery) and MLH (Metal Hydride Level). We are assuming some errors in the linear model because the current demanded for the electrolysis process or the current produced by the fuel cell varies with temperature [24]. However, a linearized model is mandatory for this controller development. The maximum error found in the comparison of the linear model versus the non-linear one was 3.14%.

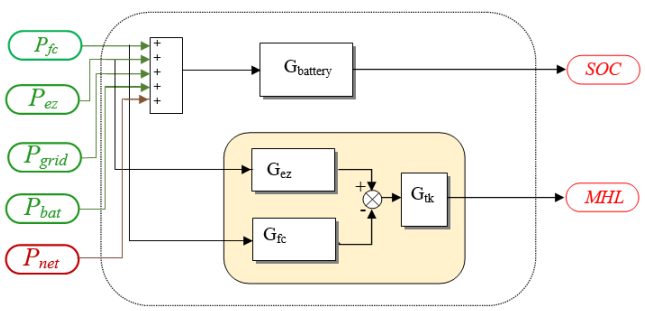

Fig. 5. Input-output of linearized model for MPC control

E. System Constraints

The system studied has physical constraints that must be taken into account during the operation. Although electrolysis is a mature technology, the electrolyzers have not been designed to operate under variable power conditions, such as those that can be found in renewable microgrids. On the other hand, fuel cells have been proven to be effective at variable power conditions, but their slow ancillary mechanisms do not always offer fast response [25]. Hence, special care must be taken when integrating this equipment into a renewable microgrid.

For safe operation, the electrolyzer should be operated above a minimum power level in order to avoid impurities in the gases produced and hazardous mixtures of H_2 in O_2. In addition, as it has been reported [6], high current densities accelerate the degradation due to overvoltage in the electrodes. Accordingly, the electrolyzer power is upper and lower bounded (8). Fuel cell carbon corrosion, as a main degradation factor, is present whenever the fuel cell is started and shut down. To limit unnecessary and frequent startups and shutdowns, a minimum demand of 100 W is required for the fuel cell operation (9). For the grid power, the amplitudes are set by the maximum allowed by the electronic source (6 kW) and load (2.5 kW) respectively (10). The battery power maximum and minimum are manufacturer recommendations (11). These constraints can be written as:

$$P_{ez,min} = 100\ \text{W} \le P_{ez} \le 900\ \text{W} = P_{ez,max} \quad (8)$$

$$P_{fc,min} = 100\ \text{W} \le P_{fc} \le 900\ \text{W} = P_{fc,\max} \quad (9)$$

$$P_{grid,min} = -2500\ \text{W} \le P_{grid} \le 6000\ \text{W} = P_{grid,\max} \quad (10)$$

$$P_{batt,\min} = -2640\ \text{W} \le \text{P}_{batt} \le 2640\ \text{W} = P_{batt,\max} \quad (11)$$

Regarding the equipment dynamics, severe load cycling in the fuel cell leads to water management and gas transport issues, which leads to further degradation of fuel cell performance and attenuation of internal parts [5]. As for the electrolyzer, among many issues, rapid fluctuations can damage the membranes irreversibly, as it has been demonstrated in [6], [7]. Furthermore, power variability can create impurities and energy losses. In summary, all these factors will increase the internal wear.

Taking into account that the electrolyzer and the fuel cell have the same membrane technology (based on PEM type) and the experience in the plant operation, the constraints related to power rates have been formulated in the same way to avoid overvoltage (electrolyzer) and undervoltage (fuel cell) issues:

$$\Delta P_{fc,\min} = -20\ W/s \le \Delta P_{fc} \le 20\ W/s = \Delta P_{fc,\max} \quad (12)$$

$$\Delta P_{ez,\min} = -20\ W/s \le \Delta P_{ez} \le 20\ W/s = \Delta P_{ez,\max} \quad (13)$$

Regarding the power rates of the grid and battery power, they are considered to have the ability to electrically respond fast enough. Thus, the constraints are set as:

$$\Delta P_{grid,\min} = -1000\ \text{W/s} \le \Delta P_{grid} \le 1000\ \text{W/s} = \Delta P_{grid,\max} \quad (14)$$

$$\Delta P_{\text{batt,min}} = -1000\ \text{W/s} \le \Delta P_{batt} \le 1000\ \text{W/s} = \Delta P_{\text{batt,max}} \quad (15)$$

According to the manufacturer, the battery bank should be operated in a limited range of SOC values in order to avoid overcharging and undercharging, which drastically reduce the total number of cycles that the battery can stand. For this study, we have considered a conservative range of SOC values (16). The metal hydride tank is not damaged from deep cycles. However, the fuel cell requires a minimum delivering pressure for the hydrogen about 2 bar. This value approximately corresponds to 10% of the hydride content. An upper bound is imposed for safety reasons. Then, the constraints related to the output variables can be written as follows:

$$SOC_{\min} = 40\ \% \le SOC \le 75\ \% = SOC_{\max} \quad (16)$$

$$MHL_{\min} = 10\ \% \le MHL \le 90\ \% = MHL_{\max} \quad (17)$$

Notice that output constraints could be considered "soft constraints", i.e. they could be surpassed. Nevertheless, the experience in the real plant operation recommends never surpassing these limits. Otherwise, the equipment lifespan will be drastically reduced. Therefore, these bounds should be considered as "hard constraints".

Equation (18) is a manufacturer constraint, which is usually given by (19). This equation has been tailored to be consistent with the system outputs (%SOC).

$$\Delta SOC_{\min} = -4.16^{-3}\ \text{SOC/s} \le \Delta SOC \le 4.16^{-3}\ \text{SOC/s} = \Delta SOC_{\max} \quad (18)$$

$$\dot{I}_{batt_{min}} = -55\,\text{A/s} \le I_{batt} \le 55\,\text{A/s} = \dot{I}_{batt_{\max}} \quad (19)$$

F. Cost function

The way the system approaches the desired behavior will be indicated by a function *J* which depends on present and future control signals:

$$J = \sum_{k=1}^{N} \delta(k)\left[\left(\hat{y}\left(t+k|t\right) - w\left(t+|k\right)\right)\right]^2 + \sum_{k=1}^{Nu} \lambda(k)\left[\left(\Delta u\left(t+k-1|t\right)\right)\right]^2 \quad (20)$$

where *u* is the future signal sequence and *w* is the sequence of the reference trajectory, λ and δ are the weighting factors. Controller goal is to obtain *u** allowable actions that minimize *J* for each sampling time. According to the control architecture presented in Fig. 3, the cost function can be rewritten as:

$$J = \sum_{k=1}^{Nu} \alpha_1 P_{fc(t+k)}{}^2 + \alpha_2 P_{ez(t+k)}{}^2 + \alpha_3 P_{grid(t+k)}{}^2 + \alpha_4 P_{batt(t+k)}{}^2 + \\ + \beta_1 \Delta P_{fc(t+k)}{}^2 + \beta_2 \Delta P_{ez(t+k)}{}^2 + \beta_3 \Delta P_{grid(t+k)}{}^2 + \beta_4 \Delta P_{batt(t+k)}{}^2 + \\ + \sum_{k=1}^{N} \gamma_1 \left(SOC_{(t+k)} - SOC_{ref} \right)^2 + \gamma_2 \left(MHL_{(t+k)} - MHL_{ref} \right)^2 \quad (21)$$

In this cost function, the first four terms weight the usage of the manipulated variables and determine the plant operation greatly. Notice that this is a multi-objective function, so the optimal solution will try to satisfy all the objectives in a weighted manner. The choice of the weights will define the priority of objectives. It is observed through simulations that the most appropriate values of the prediction horizon, control horizon and sampling time were: N=10, N_u=2 and T_s=1 s, respectively. Increasing the control horizon or the prediction horizon did not result in improved outcomes.

In the design presented, the weighting factors were tuned taking into account the technical and economic criteria enumerated in III A. These weights can be tuned by trial and error in several simulations, till the desired behavior is obtained. As a guideline, Table II summarizes the main effects that can be achieved in the microgrid, depending on the weighting factor selection. In addition to this, as a general rule, the values of each group of weights (α_i, β_i, γ_i) of the cost function are chosen according to the units of the variables (W, W/s, %) so as to keep a similar order of magnitude for each group of variables.

TABLE II
WEIGHTING FACTORS SELECTION FOR THE COST FUNCTION

Weight	Criteria	Effect
α_i	$\alpha_i > \alpha_j$	Manipulated variable associated to weight *j* is used prior to variable associated to *i*
β_i	$\beta_i > \beta_j$	Equipment associated to weight *i* is protected from intensive use more than equipment associated to weight *j*
γ_i	$\gamma_i = \gamma_j << \alpha_i, \beta_i$	System output variables are freed to follow the references, adding flexibility to the operation

Using this table, different plant behaviors can be achieved. For example, selecting $\alpha_3 >> \alpha_1$, α_2, the microgrid is operated in island mode without import/export from the local network at the expense of more intensive use of the electrolyzer and the fuel cell. Taking into account these rules, the weights of the cost function chosen for this work are presented in Table III. For further study of weights selection, a sensitivity analysis of the cost function derivate with respect to the weights can be performed. Such a study is out of the scope of this paper. The µG model needed to tune the predictive controller is fully explained in [23]. A trial-and-error approach was used to find out the cost function parameters.

TABLE III
WEIGHTING FACTORS FOR THE COST FUNCTION AND OPERATING MODES

	α_i	β_i	γ_i
x_{b1}	$[5,5,8,10^5]\cdot10^{-3}$	$[10^3, 10^3,1,1]\cdot10^{-3}$	$[1,1]\cdot10^{-3}$
x_{b2}	$[5,3,8,10^5]\cdot10^{-3}$	$[5\cdot10^3, 2\cdot10^3,1,1]\cdot10^{-3}$	$[1,1]\cdot10^{-3}$
x_{b3}	$[5,5,10,10^5]\cdot10^{-3}$	$[1\cdot10^3, 3\cdot10^3,1,1]\cdot10^{-3}$	$[1,1]\cdot10^{-3}$

As can be seen, a high weight has been assigned to P_{batt}, $(\alpha_4=10^2)$. This weight drives the controller to set this variable to zero. This is in concordance with the physical constraints, since the battery bank is not controlled directly in this microgrid due to the lack of a dedicated DC/DC converter. Notice that the weights associated to grid utilization (α_3) are higher than the fuel cell/electrolyzer weights in order to minimize power exchanged with the grid. By tuning α_i for the electrolyzer/fuel cell higher, equipment utilization and start/stops are reduced at the expense of more battery/grid usage. Power rate weights (β_1, β_2) for the fuel cell and electrolyzer have been set very high in order to protect these pieces of equipment from sudden power changes and avoid their degradation. Finally, very low values for γ_i have been chosen to allow for flexibility in the plant operation.

The weighting factors presented in Table III should be taken as indicative. They have been selected to achieve the proposed control objectives of section IIIA.

G. Model Predictive Control Formulation

The following MPC formulation is considered for the microgrid laboratory system:

$$J^*(x_k) = Min\ J$$

Subject to

power constraints (8)-(11),
power rate constraints (12)-(15),
storage constraints (16)-(17),
battery current constraints (18),

for t ϵ [k, k+N_2-1].

The optimization problem involves two optimization variables, u_k, u_{k+1}, and five parameters, $x_p=[x(1)_k, x(2)_k, v(1)_k, y(1)_{ref,k}, y(2)_{ref,k}]^T$, which correspond to the states (x), the measurable disturbance $v_k=(P_{net})$ and the storage set-points. The objective function *J* is set to minimize the quadratic norm of the error between the system output and the desired optimal profile while introducing the constraints on *u*, *v* and *y*. Thus, in this case the optimization problem is solved by multi-parametric quadratic programming (mp-QP).

H. Implementation of the Predictive Controller in the microgrid

The proposed controller has been implemented in the experimental platform described in Section II. As model-based controllers are usually high in computational demands, real-

time implementation in a commercial PLC is relatively problematic. In order to overcome this issue, the following methodology was used:

The MPC control actions are calculated using Real-time Simulink® software on a control computer installed in the plant. Using the Matlab OPC library, the computer sends these control commands to the SCADA and the PLC, which executes the orders. The MPC controller receives the plant outputs (SOC, MHL) to compute the optimal sequence of control actions.

IV. Experimental Validation of the Proposed MPC Controller

In order to verify the theoretical background, experimental tests were carried out to study the controller behavior under different external conditions (weather and demand changes). Two types of renewable sources were considered and studied separately: a PV array and a wind turbine. The demand profile was taken from a typical household daily pattern on a weekday [26] and adapted to the power scales of the laboratory microgrid. The irradiance data were gathered from Lat. 37.23 N while wind data were collected from Lat. 56.18 N.

Before testing the controller in the real plant, the controller performance should be probed in simulations. The question of a weather combination (simultaneous PV and WT) may arise at this point from the assumptions just presented. Simulations were carried out to study the external conditions impact on controller behavior. A representative simulation of the PV (Cloudy profile) plus Wind turbine is shown to demonstrate the controller reliability in any situation. Fig. 6 shows that the controller is able to effectively manage the energy in the system, using the electrolyzer, batteries and grid power.

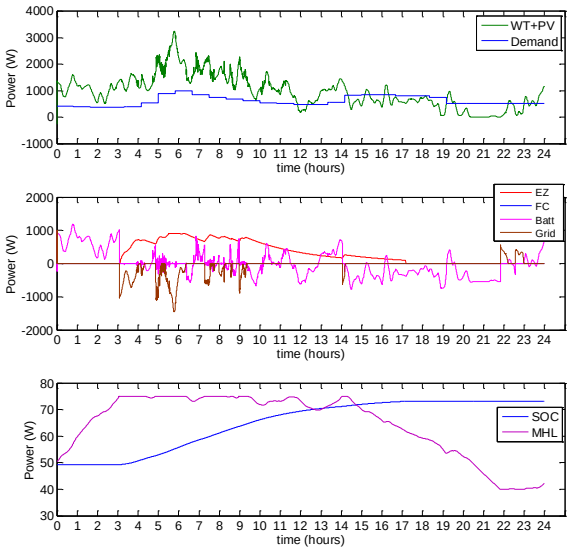

Fig. 6. Simulation example of hybrid renewable source (PV+wind turbine)

A. MPC Experimental Validation in the Sunny day scenario:

It can be observed in Fig. 7 that the electrolyzer was triggered when the battery SOC reached 75 %. The irradiance remained very high and therefore the energy needed to be stored in the form of hydrogen. The electrolyzer power consumption was increased gradually, as Fig. 7 shows. Notice that in the first moments of the electrolyzer operation, part of the excess energy was exported to the grid and gradually decreased as the electrolyzer consumed more power.

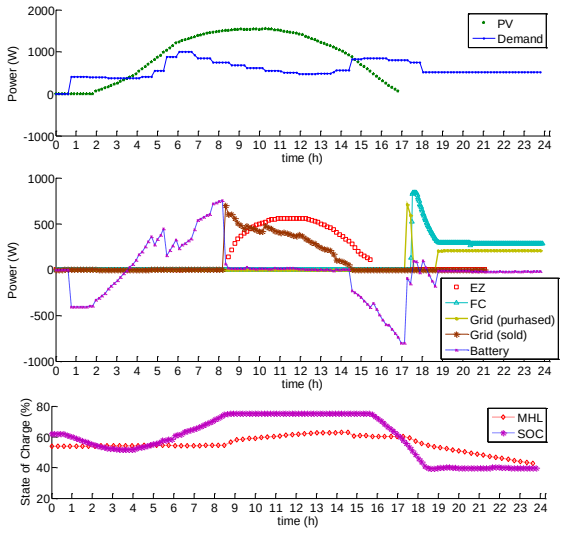

Fig. 7. Experimental results of the proposed MPC over the Sunny day test, gathered from plant operation

The fuel cell operation followed a similar pattern. It was switched on when the battery SOC reached the lower threshold (40%). The grid assumed the transient power required by the load. At the end of the day, the grid and the fuel cell shared the electricity demand according to the optimum set by the cost function. It is important to point out that the controller performance was evaluated in a wide range of operating points, varying from low to top level of battery SOC thresholds, and the performance was successful.

B. MPC Experimental Validation in the Partly Cloudy day scenario:

In the experiment results shown in Fig. 8 an energy deficit can be observed during most of the experiment hours. However, this deficit was supplied in different ways. In the first stage, when strong power fluctuations were present, the control determined that the cost of using fuel cell power is too expensive in techno-economic terms, because the high power fluctuations. Thus, the control used the grid power to satisfy the demand. In contrast, over the second stage of the experiment, the fluctuations of the cloudiness disappeared. Then, the control determined to use the fuel cell as main source to cover the demand. It is therefore confirmed that the control worked properly according to the design made.

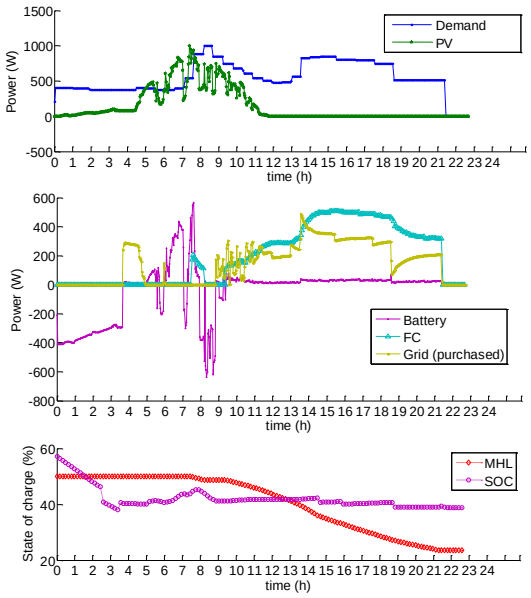

Fig. 8. Experimental results of the proposed MPC in the Partly Cloudy day test, gathered from plant operation

C. *MPC Experimental Validation in the Windy day scenario:*

In this case study, the renewable source considered was a wind turbine. The wind turbine also produced a significant power fluctuation as can be observed in Fig. 9. In this experiment, a predominant excess power motivated the electrolyzer to be working during most of the day.

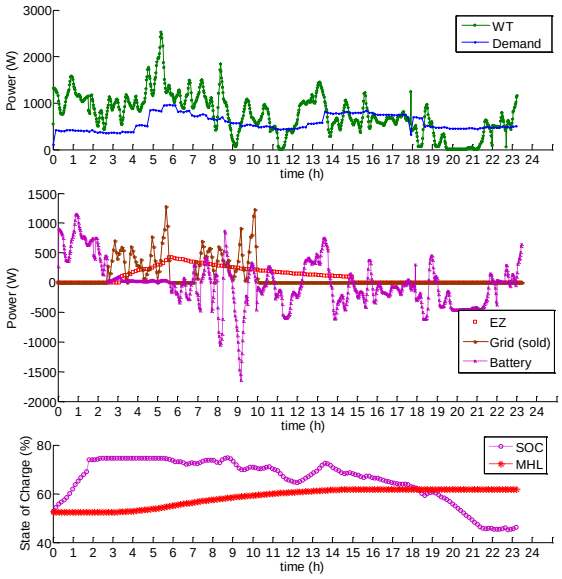

Fig. 9. Experimental results of the proposed MPC on a Windy day, gathered from plant operation

Fig. 9 shows that the operation of the proposed MPC on a Windy day was successful. Mandatory battery SOC constraints were always respected. It should be noted that the electrolyzer operation was very satisfactory. This is due to the fact that, despite the high variability of the wind power, the power rate constraints included in the controller design induced a soft equipment operation. Consequently, it was not subjected to intensive use that would greatly reduce its lifespan. The MPC controller changed the set-points gradually, according to the optimum calculated by the cost function.

V. Discussion and Benchmarking

In this section, the results obtained from the plant operation under the proposed MPC are discussed and compared against the SOC-based HB control technique, which is the most widely used strategy in H_2-µGs. In Fig. 10 we show the experimental results of HB control strategy, implemented in the same microgrid laboratory. The same load and power profiles as the MPC Partly Cloudy day experiment were used (Fig. 8).

In Fig. 10, the fuel cell is activated at steady power when the SOC reaches 40%, supplying the load and charging the batteries. This process is repeated one more time with the inefficiency involved in diverting the fuel cell power to the batteries instead of using it directly to supply the load. This intermittent operation and the ripples observed in the battery SOC can be one of the causes of the degradation mechanism that have led to the equipment premature failure in existing pilot plants. Variable power operation is an option, though in that case the drawback is that the fuel cell (or the electrolyzer) is dealing directly with the solar (or wind) fluctuations, since the net power is used as reference for the equipment. It is argued that this strategy can be another cause of premature degradation, due the PEM membranes being subjected to stress.

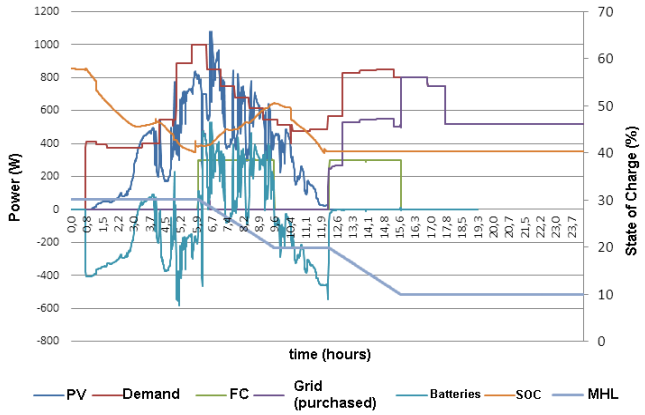

Fig. 10. Microgrid HyLab operation under HB control strategy on a Cloudy day.

In order to quantitatively compare both strategies, a group of Key Performance Indicators (KPI) were defined. Specifically: fuel cell and electrolyzer number of start-stop events, hydrogen tank and battery levels, electrolyzer and fuel cell average efficiency, equipment alarm events (power rates higher than 20-25 W/s, which may cause electrolyzer overvoltage and fuel cell undervoltage issues) and operating cost and maintenance.

The operating cost is an important indicator which takes into account the degradation of microgrid main equipment: the battery charging/discharging cycles, the fuel cell and electrolyzer degradation and the grid import-export cost of electricity is also considered by using the EEX (European Energy Exchange).

The cost of using the battery bank is measured in terms of investment cost and the power in or out of the batteries, in accordance with [27].

Regarding the electrolyzer and the fuel cell operating cost, it is expressed in (22). As their degradation mechanisms are strongly dependent on the number of start-stop events [28], such a cost has been considered to be a function of the capital cost of the equipment and the total number of start-stops that a fuel cell or an electrolyzer can stand (23). Sudden power changes also damage the equipment and have been measured in (24).

$$C_{ez,fc}^{O\&M} = \sum_{i=1}^{t} n_{on-off} C_{ez,fc}^{on-off} + C_{ez,fc}^{dP} + C_{fc}^{Voc} \quad (22)$$

$$C_{ez,fc}^{on-off} = \frac{C_{ez,fc}^{i}}{N_{ez,fc}^{on-off}} \quad (23)$$

$$C_{ez,fc}^{dP} = \left.\frac{\Delta P_{ez,fc}}{\Delta P_{ez,fc}^{\max}}\right|_{\Delta t} C_{ez,fc}^{on-off} \quad (24)$$

where C^{on-off} with subscripts *ez* and *fc* for the electrolyzer and fuel cell is the operating cost ($), n_{on-off} is a start and stop event, C^{dp} is the cost of the sudden power changes, C^{voc} (only for the fuel cell) is the cost of keeping the fuel cell at open circuit, C^{i} is the capital cost of the equipment, N^{on-off} is the total number of the start and stops that a fuel cell or an electrolyzer can stand, ΔP is the equipment power variation, ΔP_{max} is the maximum equipment power variation [0→P^{rated}] and C^{on-off} is the cost of each start and stop.

TABLE III
COMPARISON SUMMARY BETWEEN MPC AND HB OPERATIONAL RESULTS IN THREE WEATHER SCENARIOS

MPC	*HYSTERESIS BAND*
Fewer start-up/shut-downs (25% fewer)	Uncontrolled start-up/shut-downs
Variable power (smooth reference) → More energy stored (+5% MHL)	Variable power (load following) → high energy stored but also equipment damage When fixed power → low efficiency
Smooth power references (null alarm events)	Directly absorbs wind/solar fluctuations (over 200 alarms on a Cloudy day)
Higher equipment efficiency (low currents) (+3%)	Low equipment efficiency
Lower operational cost (-30%)	**Higher cost**

The purpose of these indicators is not only to benchmark control strategies, but allow system diagnosis for early fault or inadequate operation detection. The KPIs proposed can help to improve the system efficiency and reliability when testing control strategies in smartgrids, as is shown in this paper. Then, we applied the KPI described to compare the two control strategies (MPC and HB). Table III summarizes the comparison findings in the three scenarios studied.

VI. CONCLUSIONS AND FUTURE STEPS

In this paper, a MPC approach for efficient and reliable operation of a grid-connected renewable microgrid, incorporating a fuel cell and an electrolyzer as main equipment, has been presented. An implicit formulation has been used for the controller design and real-time implementation, enabling fast response to sudden disturbances in the μG. The proposed formulation includes the equipment power constraints, bounds in power rates, storage constraints, efficiency criteria and grid interaction to potentially compensate equipment early failure and therefore increase the lifespan while economically allocating the system demand. Further, a set of priority criteria for weights selection to achieve the desired behavior has been incorporated in the cost function.

The proposed approach has been investigated on a microgrid test bench located at Lat. 37.10 N. The experimental results for three typical weather patterns demonstrate that the proposed controller is able to effectively operate the plant, with the major advantage of optimal power dispatch by calculating on-line the equipment set-points under the optimization criterion.

A group of key performance indicators, which include electrolyzer and fuel cell start and stop events, equipment efficiency, fuel cell and electrolyzer alarm events and the global plant operating cost as a function of the equipment capital cost and degradation mechanisms, was defined to compare the MPC with HB technique. The benchmarking evidenced significant advantages of MPC compared with the HB strategy (which is the most common strategy in present and past H2-μG projects), such as 25% fewer start-stop events, improved efficiency of 3% and up to 5% more hydrogen stored in the tanks. As the MPC uses a cost function to minimize the power management, a dramatic reduction of 30% in operational costs is observed on average in the three scenarios studied.

Future work will focus on the development and implementation of unit commitment to determine the optimal schedule of generating units for combining long-term generation planning with present local dispatch. Other open questions are how to manage simultaneous renewable curtailment in large microgrids and other uncertainties (such as breakdowns). Incorporate fault-tolerant MPC controllers and fault detection into the work presented could help to address these issues in a common framework.

REFERENCES

[1] M. A. Zamani, T. S. Sidhu, A. Yazdani, "Investigations Into the Control and Protection of an Existing Distribution Network to Operate as a Microgrid: A Case Study," *IEEE Trans. Ind. Electron*., vol.61, no.4, pp.1904,1915, April 2014.

[2] A. Chaouachi, R.M. Kamel, R. Andoulsi, K. Nagasaka, "Multiobjective Intelligent Energy Management for a Microgrid," *IEEE Trans. Ind. Electron.*, vol.60, no.4, pp.1688,1699, April 2013.
[3] L. Valverde, D. Ali, M. Abdel-Wahab, J. Guerra and D. Hogg, "A technical evaluation of Wind-Hydrogen (WH) demonstration projects in Europe," *in Proc. IEEE POWERENG*, Istanbul, 2013.
[4] Ø. Ulleberg, H. Ito, M. R. B. Maack, S. Miles, N. Kelly, A. Iacobazzi, M. Argumosa, S. Schoenung and E. Stewart, "Hydrogen demonstration projects evaluation," IEA agreement on the Production and Utilization of Hydrogen., 2009.
[5] N. v. Dijk, "Pem Electrolyser degradation mechanisms and practical solutions," in Durability and Degradation Issues in PEM Electrolysis Cells and its Components, Freiburg, 2013.
[6] P. Pei and H. Chen, "Main factors affecting the lifetime of Proton Exchange Membrane fuel cells in vehicle applications: A review," Appl. Energy, vol. 125, no. 0, pp. 60-75, 2014.
[7] F. Barbir, "PEM electrolysis for production of hydrogen from renewable energy sources," Solar Energy, Volume 78, Issue 5, pp. Pages 661-669, 2005
[8] Ø. Ulleberg, "The importance of control strategies in PV–hydrogen systems," Solar Energy, vol. 76, no. 1-3, pp. 323-329, 2004.
[9] D. Ipsakis, S. Voutetakis, P. Seferlis, F. Stergiopoulos and C. Elmasides, "Power management strategies for a stand-alone power system using renewable energy sources and hydrogen storage," Int J Hydrogen Energy, vol. 16, no. 34, pp. 7081-7095, 2009.
[10] A. Bemporad, F. Borrelli and M. Morari, "Model predictive control based on linear programming - the explicit solution," *IEEE Trans. on Automatic Control.*, vol. 47, no. 12, pp. 1974-1985, 2002.
[11] D. Ipsakis, S. Voutetakis, P. Seferlis, F. Stergiopoulos, S. Papadopoulou and C. Elmasides, "The effect of the hysteresis band on power management strategies in a stand-alone power system," Energy, vol. 33, no. 10, pp. 1537-1550, 2008.
[12] C. Ziogou, D. Ipsakis, C. Elmasides, F. Stergiopoulos, S. Papadopoulou, P. Seferlis and S. Voutetakis, "Automation infrastructure and operation control strategy in a stand-alone power system based on renewable energy sources," J.Power Sources, vol. 196, no. 22, pp. 9488-9499, 2011.
[13] M. Little, M. Thomson and D. Infield, "Electrical integration of renewable energy into stand-alone power supplies incorporating hydrogen storage," Int J Hydrogen Energy, vol. 32, no. 10-11, pp. 1582-1588, 2007.
[14] P. Zervas, H. Sarimveis, J. Palyvos and N. Markatos, "Model-based optimal control of a hybrid power generation system consisting of photovoltaic arrays and fuel cells," Journal of Power sources, vol. 181, no. 2, pp. 327-338, 2008.
[15] M. Khalid and A. Savkin, "A model predictive control approach to the problem of wind power smoothing with controlled battery storage," Renewable Energy, vol. 35, no. 7, pp. 1520-1526, 2010.
[16] A. del Real, A. Arce y C. Bordons, "Hybrid model predictive control of a two-generator power plant integrating photovoltaic panels and Fuel Cell," *in Proc. IEEE Conf. on Decision and Control*, New Orleans, 2007.
[17] M. Korpås and A. T. Holen, "Operation planning of hydrogen storage connected to wind power operating in a power market," *IEEE Trans. on Energy Convers.*, vol. 21, no. 3, pp. 742-749, 2006.
[18] M. Pereira, D. Limon, T. Alamo, L. Valverde, C. Bordons, "Economic model predictive control of a smartgrid with hydrogen storage and PEM fuel cell," *in Proc. IEEE IECON*, Vienna, 2013.
[19] M. Trifkovic, M. Sheikhzadeh, K. Nigim and P. Daoutidis, "Modeling and Control of a Renewable Hybrid Energy System With Hydrogen Storage," *IEEE Trans. Control Syst. Technol.*, vol. 22, no. 1, pp. 169-179, 2014.
[20] A. Parisio, E. Rikos, G. Tzamalis and L. Glielmo, "Use of model predictive control for experimental microgrid optimization," Appl. Energy, 2014, 115, 0, vol. 115, no. 0, pp. 37-46, 2014.
[21] L. Valverde, F. Rosa and C. Bordons, "Design, Planning and Management of a Hydrogen-Based Microgrid," *IEEE Trans. on Industrial Informat.*, vol. 9, no. 3, pp. 1398-1404, 2013.
[22] A. Bidram and A. Davoudi, "Hierarchical Structure of Microgrids Control System," *IEEE Trans. Smart Grid*, vol. 3, no. 4, pp. 1963-1976, 2012.
[23] L. Valverde, F. Rosa, A. del Real, A. Arce and C. Bordons, "Modeling, simulation and experimental set-up of a renewable hydrogen-based domestic microgrid," Int J Hydrogen Energy, vol. 38, no. 27, pp. 11672-11684, 2013.
[24] F. Pino, L. Valverde and F. Rosa, "Influence of wind turbine power curve and electrolyzer operating temperature on hydrogen production in wind–hydrogen systems," J.Power Sources, vol. 196, no. 9, pp. 4418-4426, 2011.
[25] M. H. Nehrir y C. Wang, "Modeling and control of fuel cells. Distribute Generation Applications", *IEEE Press Series on Power Engineering*, 2009.
[26] G. Sara and B. Guenther, "User behavior and patterns of electricity use for energy saving," in 6th Internationale Energiewirtschaftstagung an der TU Wien, Vienna, 2009.
[27] R. Dufo-López, J. L. Bernal-Agustín and F. Mendoza, "Design and economical analysis of hybrid PV–wind systems connected to the grid for the intermittent production of hydrogen," Energy Policy, vol. 37, no. 8, p. 3082–3095, 2009.
[28] E. Zakrisson, "The Effect of Start/Stop strategy on PEM fuel cell degradation Charasteristics," M.S. thesis, Gothenburg, Sweden, 2011.

Luis Valverde received his Ph.D in Industrial Engineering in November 2013 from the University of Seville, Spain, where he is currently working as Technical Manager of HyLab laboratory. He joined the Energy Engineering group in 2007, where he was responsible for the designing and commissioning of the renewable energy laboratory: HyLab (2007–2010) funded by the Ministry of Science and Technology. His research experience comprises renewable energy generation and storage, including diverse storage technologies, such as batteries, hydrogen, super-capacitors and flywheels. He has worked in several national and international research projects in collaboration with the Systems Engineering and Automatic Control department, combining his experience in the energy field with advanced control techniques. He is author and coauthor of fifteen technical papers.

Carlos Bordons (M'98) received the Ph.D. degree in electrical engineering in 1994. He then joined, as an Assistant Professor, the Escuela Tecnica Superior de Ingeniería, University of Seville, Spain, where he is currently Full Professor of Systems Engineering and Automatic Control and the Head of the Systems Engineering and Automatic Control Department. He coauthored the books *Model Predictive Control in the Process Industry* and *Model Predictive Control* (first and second editions) published by Springer-Verlag, London. He is the holder of two related patents. His current research interests include advance process control, particularly model predictive control and its application to energy systems. His recent work is focused on power management in hybrid vehicles and control of microgrids, including renewable sources. Prof. Bordons was elected as a Council Member of the European Union Control Association in 2007. He is currently an Associate Editor of the IEEE Transactions on Industrial Electronics and Control Engineering Practice.

Felipe Rosa received the Ph.D. degree in 2003 from the Universidad de Seville, Seville, Spain. He was head of Energy Lab of INTA between 1996 and 2008. Main topics of its research are integration of renewable energies and hydrogen technologies production, hydrogen storage and fuel cell. He leads several international and national R&D projects in the fields of solar thermal plants, hydrogen production, hydrogen storage and fuel cell. He is author of more than twenty technical papers. He received the award of "City of Seville" in 2004.